CFD ANALYSIS OF NATURAL CONVECTION IN A VERTICAL MICROCHANNEL

A THESIS SUBMITTED IN PARTIAL FULFILLMENT OF THE REQUIREMENTS FOR THE DEGREE OF

Bachelor of Technology

In

Mechanical Engineering

By

ASHISH KUMAR

Department of Mechanical Engineering

National Institute of Technology

Rourkela, Orissa

2009

CFD ANALYSIS OF NATURAL CONVECTION IN A VERTICAL MICROCHANNEL

A THESIS SUBMITTED IN PARTIAL FULFILLMENT

OF THE REQUIREMENTS FOR THE DEGREE OF

Bachelor of Technology

In

Mechanical Engineering

By

ASHISH KUMAR

Under the Guidance of

Prof. S. K. Mahapatra

Department of Mechanical Engineering

National Institute of Technology

Rourkela, Orissa

2009

National Institute of Technology

Rourkela

CERTIFICATE

This is to certify that the thesis entitled, "CFD ANALYSIS OF NATURAL CONVECTION IN A VERTICAL MICROCHANNEL", submitted by **Mr. Ashish Kumar** in partial fulfillment of the requirements for the award of Bachelor of Technology Degree in Mechanical Engineering at the National Institute of Technology, Rourkela (Deemed University) is an authentic work carried out by him under my supervision and guidance.

To the best of my knowledge, the matter embodied in the thesis has not been submitted to any other University / Institute for the award of any Degree.

Date:……

Prof. S. K. Mahapatra
Mechanical Engineering
NIT ROURKELA

ACKNOWLEDGEMENT

The satisfaction and euphoria on the successful completion of any task would be incomplete without the mention of the people who made it possible whose constant guidance an encouragement crowned out effort with success.

I am grateful to the **Dept. of Mechanical Engineering, NIT ROURKELA,** for giving me the opportunity to execute this project, which is an integral part of the curriculum in B.Tech programme at the National Institute of Technology, Rourkela.

I would also like to take this opportunity to express heartfelt gratitude for my project guide **Prof. S.K. Mahapatra,** who provided me with valuable inputs at the critical stages of this project execution.

I would like to acknowledge the support of every individual who assisted me in making this project a success.

Date:…….

ASHISH KUMAR
B.Tech (10503067)
Dept. of Mechanical Engg.

CONTENTS

1. ABSTRACT:

It is highly desirable to understand the fluid flow and the heat transfer characteristics of buoyancy-induced micropump and microheat exchanger in microfluidic and thermal systems. In this study, we analytically investigate the fully developed natural convection in an open-ended vertical parallel-plate microchannel with asymmetric wall temperature distributions. Both of the velocity slip and the temperature jump conditions are considered because they have countereffects both on the volume flow rate and the heat transfer rate. Results reveal that in most of the natural convection situations, the volume flow rate at microscale is higher than that at macroscale, while the heat transfer rate is lower. It is, therefore, concluded that the temperature jump condition induced by the effects of rarefaction and fluid-wall interaction plays an important role in slip-flow natural convection. Certain assumptions made during the analysis neglecting the entrance region heat and mass exchange are also validated.

2. INTRODUCTION

Convective heat transfer is a mechanism of heat transfer occurring because of bulk motion (observable movement) of fluids. As convection is dependent on the bulk movement of a fluid it can only occur in liquids, gases and multiphase mixtures. Convective heat transfer is split into two categories: natural (or free) convection and forced (or advective) convection, also known as heat advection.

Natural convection is a mechanism, or type of heat transport in which the fluid motion is not generated by any external source (like a pump, fan, suction device, etc.) but only by density differences in the fluid occurring due to temperature gradients. In natural convection, fluid surrounding a heat source receives heat, becomes less dense and rises. The surrounding, cooler fluid then moves to replace it. This cooler fluid is then heated and the process continues, forming a convection current; this process transfers heat energy from the bottom of the convection cell to top. The driving force for natural convection is buoyancy, a result of differences in fluid density. Because of this, the presence of a proper acceleration such as arises from resistance to gravity, or an equivalent force (arising from acceleration, centrifugal force or Coriolis force), is essential for natural convection.

Mathematically, the tendency of a particular system towards natural convection relies on the Grashof number (Gr), which is a ratio of buoyancy force and viscous force.

$$Gr = \frac{g\beta\Delta T L^3}{\nu^2}$$

The relative magnitudes of the Grashof and Reynolds number determine which form of convection dominates, if

$$\frac{Gr}{Re^2} \gg 1$$

forced convection may be neglected, whereas if

$$\frac{Gr}{Re^2} \ll 1$$

natural convection may be neglected. If the ratio is approximately one both forced and natural convection need to be taken into account.

Microelectromechanical systems (MEMS) based devices find their applications in a wide variety of emerging technologies, ranging from the microactuators, microsensors, microreactors to the microchannel heat sinks and the thermo-mechanical data storage systems, to name a few. Design and optimization of many of these microdevices involve the analysis of gas flows through microfluidic conduits, thereby emphasizing the need for reliable and efficient mathematical models to address the issues of coupled flow physics and heat transfer over the reduced length scales. Microfluidic systems typically have characteristic lengths of the order of 1–100 μm.

The primary challenges associated with the computational analysis of microscale gaseous flows originate from the fact that the flow physics tend to get changed altogether, as one reduces the length scales from the macro domain to the micro domain. The classical continuum hypothesis ceases to work as the distance traversed by molecules between successive collisions (i.e., the mean free path, k)becomes comparable with the characteristic length scale of the system (D)over which characteristic changes in the transport phenomena are expected to occur. The ratio of these two quantities, known as the Knudsen number (Kn = k/D), is an indicator of the degree of rarefaction of the system, which determines the extent of deviation from a possible continuum behaviour (see Fig. 1). For

$$0< Kn < 0.01,$$

the flow domain can be treated as a continuum, in which the Navier Stokes equation in conjunction with the no-slip wall boundary conditions become applicable. On the other extreme, when

$$Kn > 10,$$

the flow becomes free molecular in nature, because of negligible molecular collisions. The range of

$$0.01< Kn < 0.1$$

is known as the slip flow regime, over which the no slip boundary condition becomes invalid, although continuum conserva-tion equations can still be used to characterize the bulk flow. However, over the Kn range of 0.1–1 (the so called transitional regime), the continuum hypothesis progressively ceases to work altogether, thereby necessitating a shift of paradigm from the continuum-based modeling to particle-based modeling. Although this classification is based on empirical information and the strict demarcating limits between the different flow regimes may depend on the specific problem geometry [1–3], it essentially offers with a qualitative criterion based on which appropriate mathematical models can be chosen for the thermo-fluid analysis, consistent with the underlying physical picture. In this context, it is also important to re-iterate that in micro-scale gas flows, thermodynamic equilibrium may not prevail at the fluid–solid interface.

Accordingly, a finite velocity slip and temperature jump may need to be accounted for at the fluid–solid interface [1–6]. Depending on the degree of rarefaction of gaseous flows in micro-scale geometries, appropriate physics needs to be incorporated in the mathematical model to accommodate these effects. It has been well established by various researchers [2], [3] and [7] that the traditional Navier Stokes equations, coupled with velocity slip and temperature jump conditions at the fluid–solid interface, can simulate gaseous flows in micro-scales to a high degree of accuracy in the slip flow regimes. For transition and free molecular flow regimes, however, particle based methods such as the Direct Simulation Monte Carlo (DSMC) need to be adopted [1].

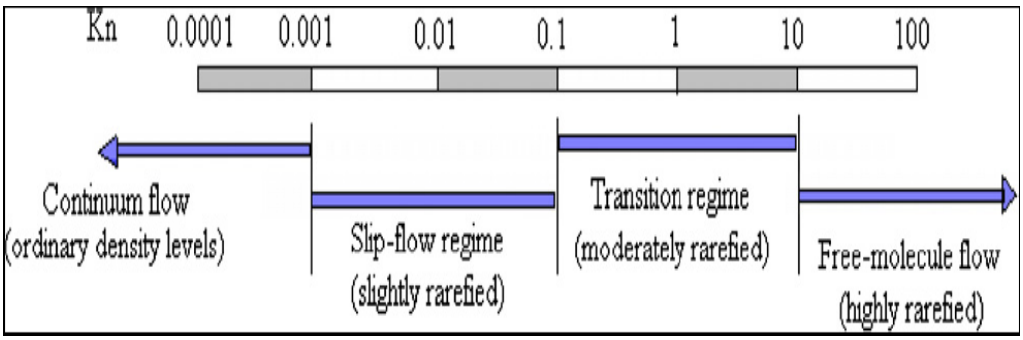

Fig. 1. Gas flow regimes based on Knudsen number.

3.LITERATURE REVIEW

Although a vast body of literature exits on the forced convection gas flows in micro-systems, only a few studies have been reported so far on natural convection in vertical microchannels.

A classi-fication of different flow regimes based on Kn (as shown in fig.1) is given in Schaaf & Chambre [1]. Here, we concern ourselves with a rarefied gas considered near the continuum region in the range $10^{-2} < Kn < 10^{-1}$, the so-called slip flow. Using the Navier–Stokes equations, Arkilic et al. [2] and Liu et al. [3] found that the theoretical results for some microflows would fit the experimental data as the slip-flow condition induced by rarefaction effect is considered.

More recently, Larrode et al. [4] and Yu and Ameel [5] considered the temperature jump condition and found that the effect of fluid-wall interaction is also important. Natural convection of an enclosed fluid has received considerable attention in recent years due to its wide applications in engineering problems. Earlier work on this problem in isothermal parallel-plate channels was experimentally reported by Elenbaas [6]. Further investigations have been carried out for different thermal boundary conditions. An excellent review was given in the book Gebhart et al. [7]. It should be noted that Aung [8] has studied the macroscale problem. All of the previous investigations were conducted at macroscale. A study on natural convection flow in microscale systems should be studied extensively.

4.A brief introduction to CFD:

Computational fluid dynamics (CFD) is one of the branches of mechanics that uses numerical methods and algorithms to solve and analyze problems that involve fluid flows and heat transfer. Computers are used to perform the millions of calculations required to simulate the interaction of liquids and gases with surfaces defined by boundary conditions. Even with high-speed supercomputers only approximate solutions can be achieved in many cases.

The fundamental basis of any CFD problem are the Navier-Stokes equations, which define any single-phase fluid flow. These equations can be simplified by removing terms describing viscosity to yield the discretised algebraic equations.

Any governing differential equation is broken down into simple algebraic equations which can then be solved iteratively using computers. The 3 basic method of discretisation are:

i) Finite difference method (FDM)
ii) Finite volume method (FVM)
iii) Finite element method (FEM)

i) Finite Difference Method (FDM):

Finite-difference methods are numerical methods for approximating the solutions to differential equations using finite difference equations to approximate derivatives.

Finite-difference methods approximate the solutions to differential equations by replacing derivative expressions with approximately equivalent difference quotients. That is, because the first derivative of a function f is, by definition,

$$f'(a) = \lim_{h \to 0} \frac{f(a+h) - f(a)}{h},$$

then a reasonable approximation for that derivative would be to take

$$f'(a) \approx \frac{f(a+h) - f(a)}{h}$$

for some small value of h. In fact, this is the forward difference equation for the first derivative. Using this and similar formulae to replace derivative expressions in differential equations, one can approximate their solutions without the need for calculus.

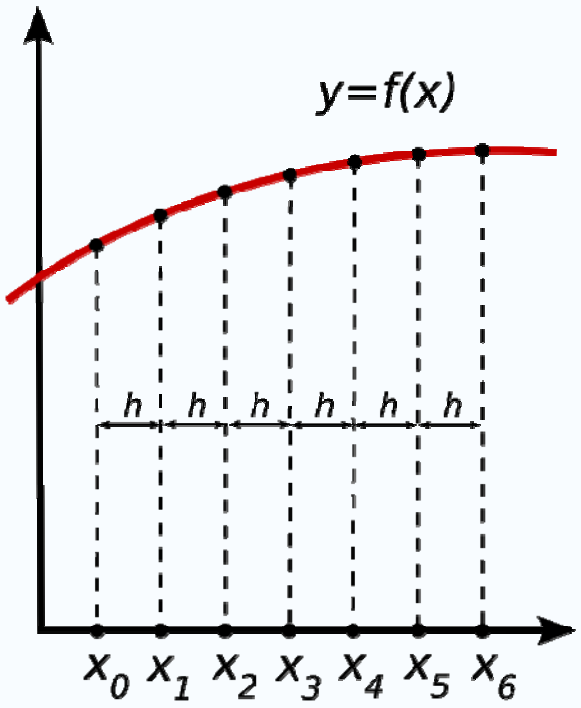

ii) Finite Volume Method:

The **finite volume method** is a method for representing and evaluating partial differential equations as algebraic equations [LeVeque, 2002; Toro, 1999]. Similar to the finite difference method, values are calculated at discrete places on a meshed geometry. "Finite volume" refers to the small volume surrounding each node point on a mesh. In the finite volume method, volume integrals in a partial differential equation that contain a divergence term are converted to surface integrals, using the divergence theorem. These terms are then evaluated as fluxes at the surfaces of each finite volume. Because the flux entering a given volume is identical to that leaving the adjacent volume, these methods are conservative. Another advantage of the finite volume method is that it is easily formulated to allow for unstructured meshes.

Control volume

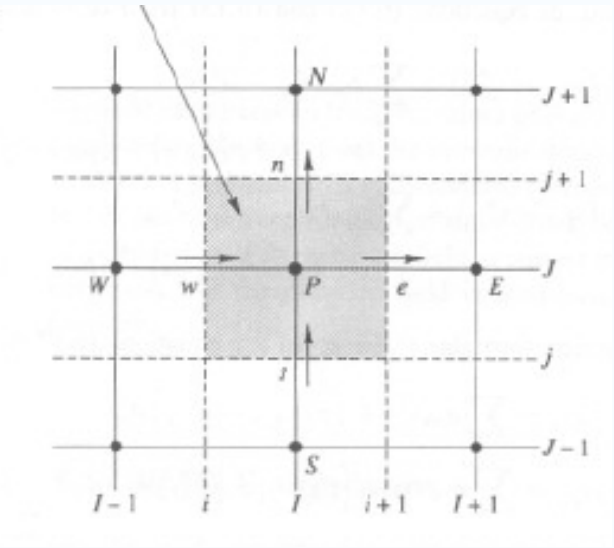

The workspace is divided into control volumes and discretisation is done by integrating over the control volume.

iii) Finite Element Method:

The **finite element method (FEM)** (sometimes referred to as **finite element analysis**) is a numerical technique for finding approximate solutions of partial differential equations (PDE) as well as of integral equations. The solution approach is based either on eliminating the differential equation completely (steady state problems), or rendering the PDE into an approximating system of ordinary differential equations, which are then numerically integrated using standard techniques such as Euler's method, Runge-Kutta, etc.

In solving partial differential equations, the primary challenge is to create an equation that approximates the equation to be studied, but is numerically stable, meaning that errors in the input data and intermediate calculations do not accumulate and cause the resulting output to be meaningless. There are many ways of doing this, all with advantages and disadvantages. The Finite Element Method is a good choice for solving partial differential equations over complex domains (like cars and oil pipelines), when the domain changes (as during a solid state reaction with a moving boundary), when the desired precision varies over the entire domain, or when the solution lacks smoothness.

5.PROBLEM FORMULATION

The problem was formulated in 2 parts. In the first part analysis was done for hydro dynamically fully developed condition. In the second part of problem formulation a more general approach was adopted to analyse the conditions in the entrance region of the microchannel.

a) Hydro dynamically fully developed analysis:

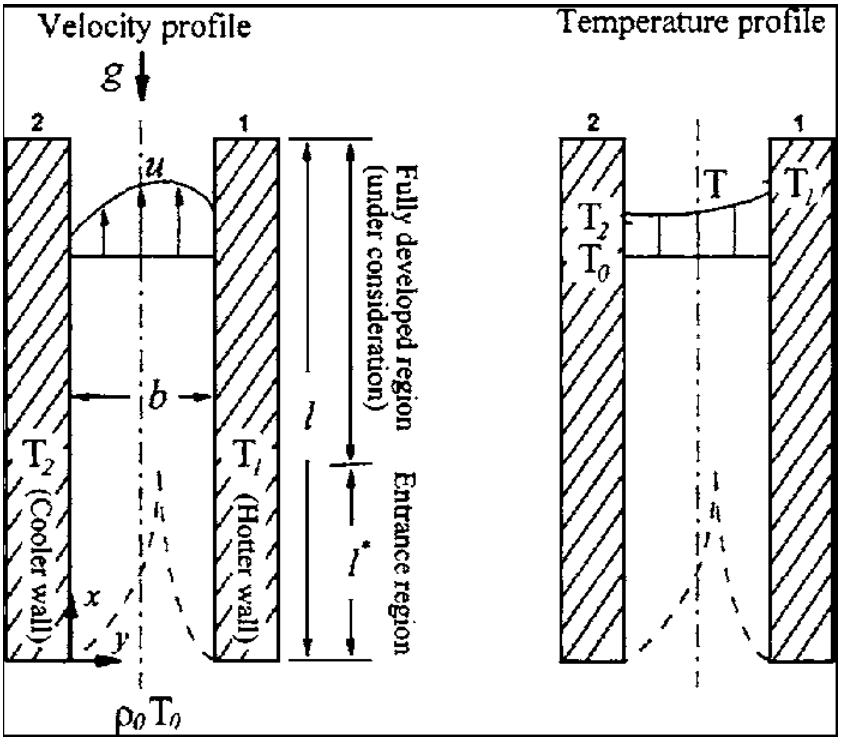

Fig. 2 Geometric sketch and parameters of natural convection in the microchannel

A vertical parallel-plate microchannel of a width b, whose temperatures of the hotter and cooler plates are T1 and T2, respectively was considered. Both ends of the channel are open to the ambient of density ρ_0 as shown in Fig. 2. Let x and y denote the usual rectangular coordinates, and let u and v denote the components of velocity field. Here constant physical properties are considered, internal heat generations are neglected, and the effect of compressibility for this typically low-speed microflow is negligible
[9]. Under the usual Boussinesq approximation, the boundary layer equations described by continuity equation, momentum equation, and energy equation for two-dimensional steady flow with gravitational acceleration g are [10].

Continuity:

$$\frac{\partial u}{\partial x} + \frac{\partial v}{\partial y} = 0, \qquad (1)$$

X-Momentum:

$$\rho_0 \left(u\frac{\partial u}{\partial x} + v\frac{\partial u}{\partial y} \right) = -\frac{d\hat{p}}{dx} + \rho_0 g\beta(T - T_0) + \mu\frac{\partial^2 u}{\partial y^2}, \quad (2)$$

Energy:

$$\rho_0 c\left(u\frac{\partial T}{\partial x}+v\frac{\partial T}{\partial y}\right)=k\frac{\partial^2 T}{\partial y^2}+\mu\left\{2\left[\left(\frac{\partial u}{\partial x}\right)^2+\left(\frac{\partial v}{\partial y}\right)^2\right]+\left(\frac{\partial u}{\partial y}+\frac{\partial v}{\partial x}\right)^2\right\}, \quad (3)$$

where is the thermal expansion coefficient, is the dynamic viscosity, c is the specific heat, k is the thermal conductivity, **p** is the pressure defect, T is the temperature, and T0 is the free stream temperature. Now we assume that the **hydrodynamically fully developed condition:**

- **i)** $\partial u/\partial x=0$,
- **ii)** $v=0$, and
- **iii)** $\partial p/\partial x=0$

can be achieved after the fluid reaches the position **y= l*** . The dimensionless governing equations are

$$\frac{d^2U}{dY^2}=-\Theta, \quad (4)$$

$$\mathrm{Ra}U\frac{\partial\Theta}{\partial X}=\frac{\partial^2\Theta}{\partial Y^2}+\mathrm{Br}\left(\frac{dU}{dY}\right)^2, \quad (5)$$

Where,

$$X = \frac{x}{b},\ Y = \frac{y}{b},\ U = \frac{u}{U_c},\ \Theta = \frac{T-T_0}{T_1-T_0},$$
$$\mathrm{Ra} = \frac{\rho_0 c U_c b}{k},\ \mathrm{Br} = \frac{\mu U_c^2}{k(T_1-T_0)},\ U_c = \frac{\rho_0 g\beta(T_1-T_0)b^2}{\mu}. \quad (6)$$

A solution of Eq. (4) in the form U(Y) is only possible if Θ is a function of Y position only, i.e., $\partial\Theta/\partial X=0$. It implies that the assumption of a **hydrodynamically fully developed natural convection necessarily means that the natural convection is also thermally fully developed**. Moreover, Br is known as the Brinkman number and is a characteristic dimensionless parameter for viscous dissipation. For rarefied gaseous micronatural convection (typically low-speed flow and low-Prandtl-number fluid), viscous dissipation term is negligible relative to the $d^2\Theta/dY^2$ term. The modified dimensionless energy equation then becomes,

$$\frac{\partial^2\Theta}{\partial Y^2} = 0. \quad (7)$$

The boundary conditions which describe velocity slip and temperature jump conditions at the fluid-wall interface are [11][12][13],

$$U(0) = \beta_v \mathrm{Kn}\frac{dU(0)}{dY},\ U(1) = -\beta_v \mathrm{Kn}\frac{dU(1)}{dY},$$
$$\Theta(0) = \xi + \beta_v \mathrm{Kn}\ In\frac{\partial\Theta(0)}{\partial Y},\ \Theta(1) = 1 - \beta_v \mathrm{Kn}\ In\frac{\partial\Theta(1)}{\partial Y}, \quad (8)$$

Where,

$$\beta_v = \frac{2 - F_v}{F_v}, \quad \beta_t = \frac{2 - F_t}{F_t} \frac{2\gamma_s}{\gamma_s + 1} \frac{1}{\mathrm{Pr}}, \quad \mathrm{Kn} = \frac{\lambda}{b}$$

$$In = \frac{\beta_t}{\beta_v}, \quad \xi = \frac{T_2 - T_0}{T_1 - T_0}. \qquad (9)$$

Here γ_s is the ratio of specific heats, Pr is the Prandtl number, F_v and F_t are the tangential momentum and thermal accommodation coefficients, respectively, and range from near 0 to 1, λ is the molecular mean free path, Kn is the Knudsen number, *In* is the fluid-wall interaction parameter, and ξ is the wall-ambient temperature difference ratio. Referring to the values of F_v and F_t given in Eckert and Drake [11] and Goniak and Duffa [13], the value of β_v is near unity, and the value of β_t ranges from near 1 to more than 100 for actual wall surface conditions and is near 1.667 for many engineering applications, corresponding to F_v=1, F_t=1, γ_s=1.4, and Pr=0.7(β_v=1, β_t=1.667).

Eq.(4) and eq.(7) are the governing equations and are numerically modelled using Computational Fluid Dynamics (CFD) approach.

The equations were discretised using Finite Difference Method.

$$\frac{d^2U}{dY^2} = -\Theta,$$

$$\frac{\partial^2\Theta}{\partial Y^2} = 0.$$

Eq. (7):

$(\partial^2\Theta/\partial Y^2) = (\Theta(i+1) + \Theta(i-1) - 2*\Theta(i)) / (\delta Y)^2 = 0$

$$\boldsymbol{\Theta\ (i) = (\Theta(i+1) + \Theta(i-1))/2}$$

Similarly Eq. (4)

$(\partial^2 U/\partial Y^2) = (U(i+1) + U(i-1) - 2*U(i)) / (\delta Y)^2 = - \Theta$

$$\boldsymbol{U(i) = U(i+1) + U(i-1) + \Theta\ (i) * (\delta Y)^2}$$

These 2 discretised equations are solved iteratively using Gauss Siedel method. Since the analysis turns out to be one dimensional the channel width is divided into 100 subdivisions. Boundary conditions as given by Eq. (8) and Eq. (9) are incorporated at the walls. A tolerance limit of 10^{-5} is adopted. A grid independence test is carried out and it is found that after a grid size of 30 the results hardly differ.

Following results were obtained which were then validated with those results obtained by Chen & Wang. The results were seen to almost coincide with all of those obtained by Chen and Wang.

Following are the results obtained for different conditions:

i) In = 1.667

a) ξ=-1, β_vKn=0

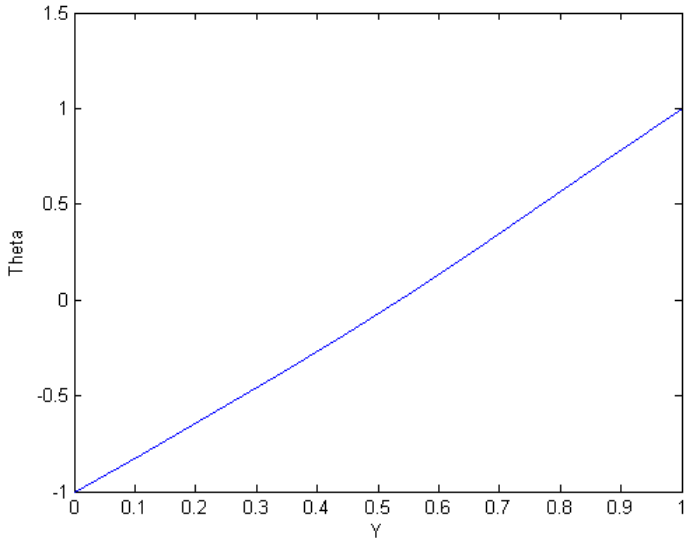

b) ξ=-1, β_vKn=0.05

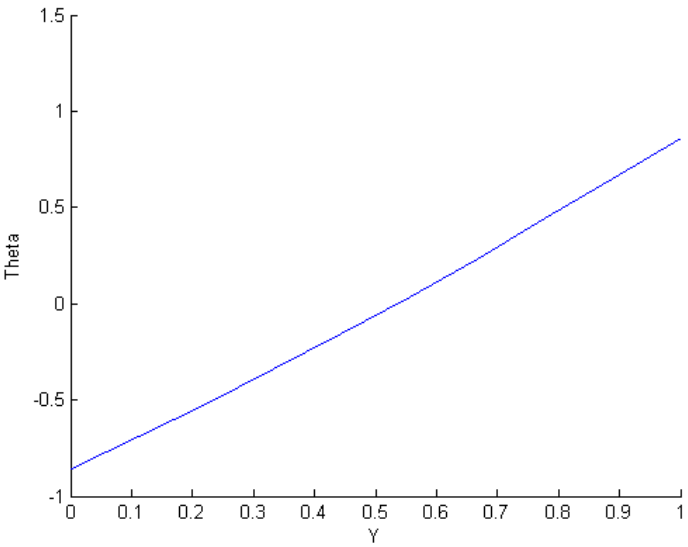

c) ξ=-1, β_vKn=0.1

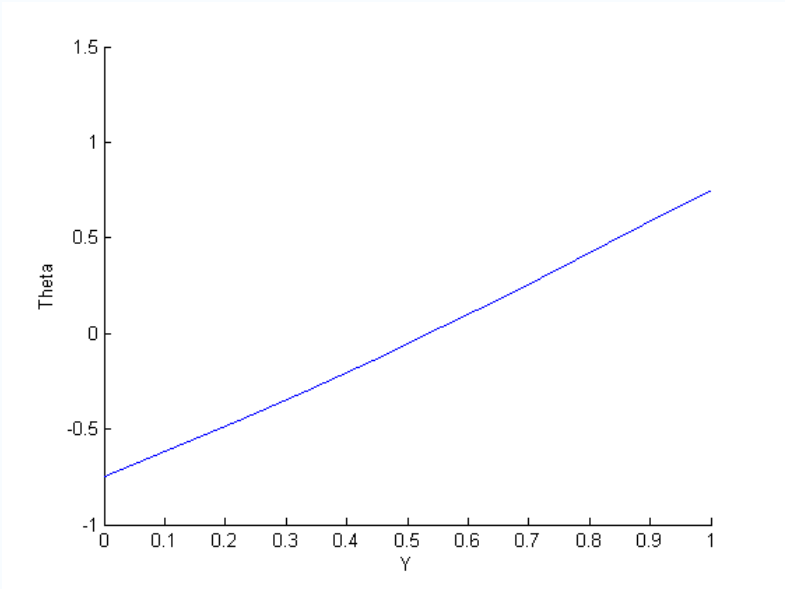

e) ξ=0, β_vKn=0.05

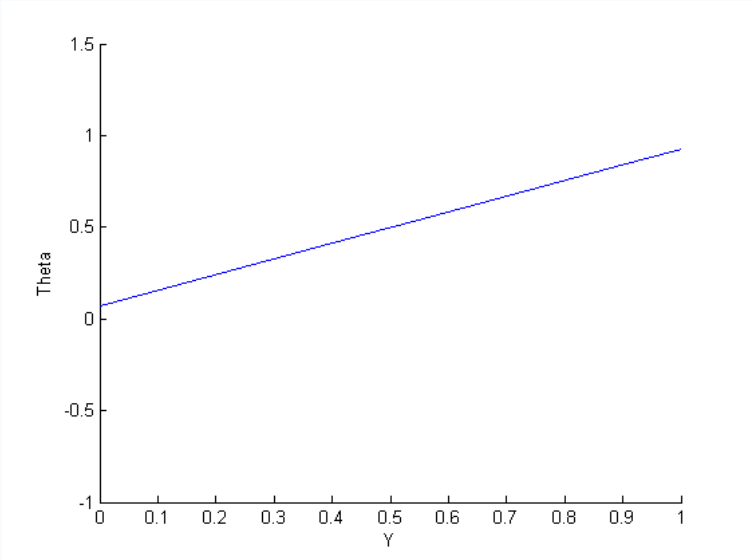

f) $\xi=0$, $\beta_v Kn=0.1$

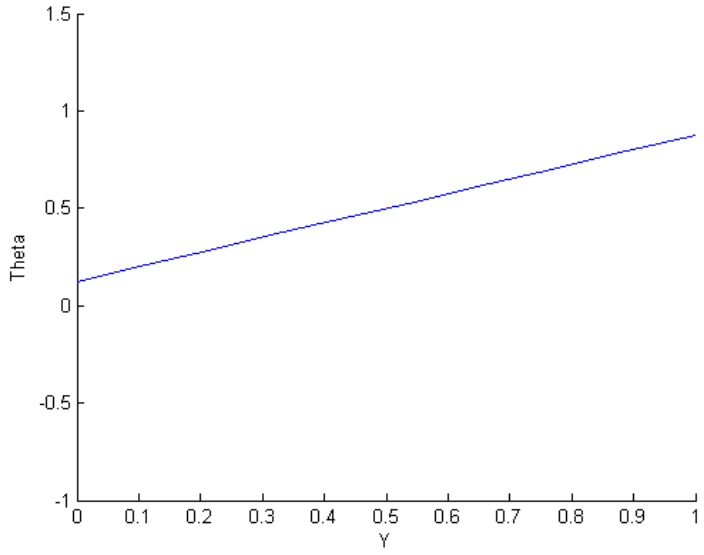

g) $\xi=1$, $\beta_v Kn=0, 0.05, 0.1$

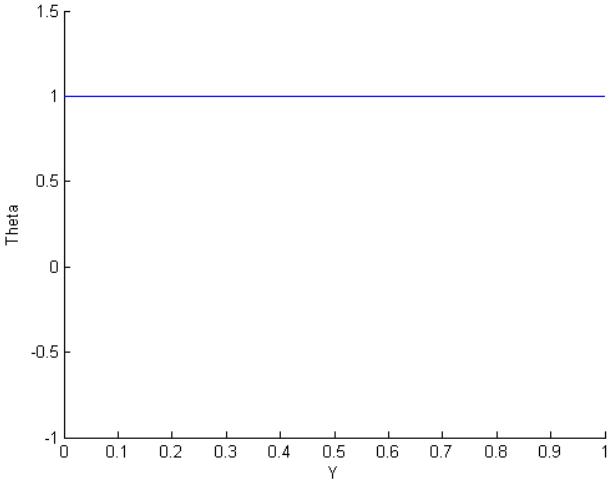

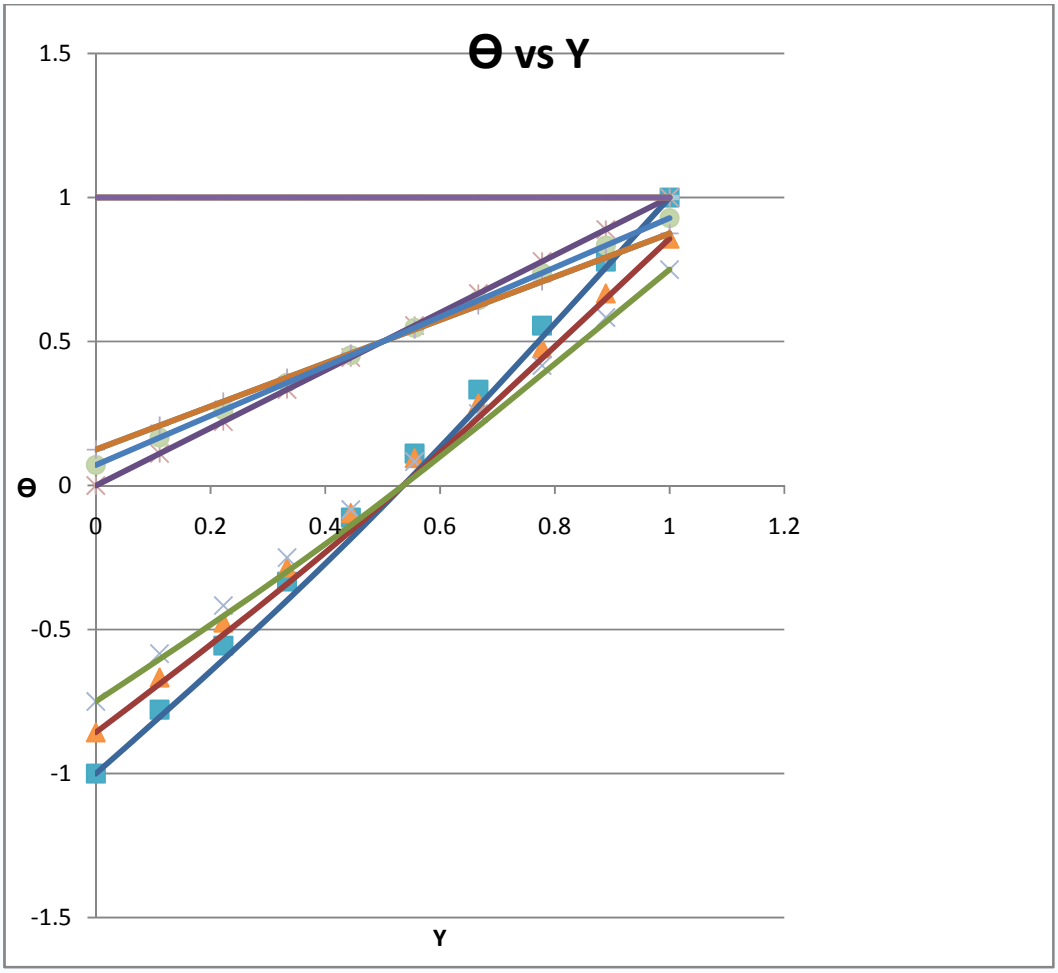

Fig.A

This is the overall graph of the above conditions where the highlighted points represent the actual values as per Chen and Wang.

ii)$\beta_v Kn=0.05$

a) $\xi=-1$, In=0

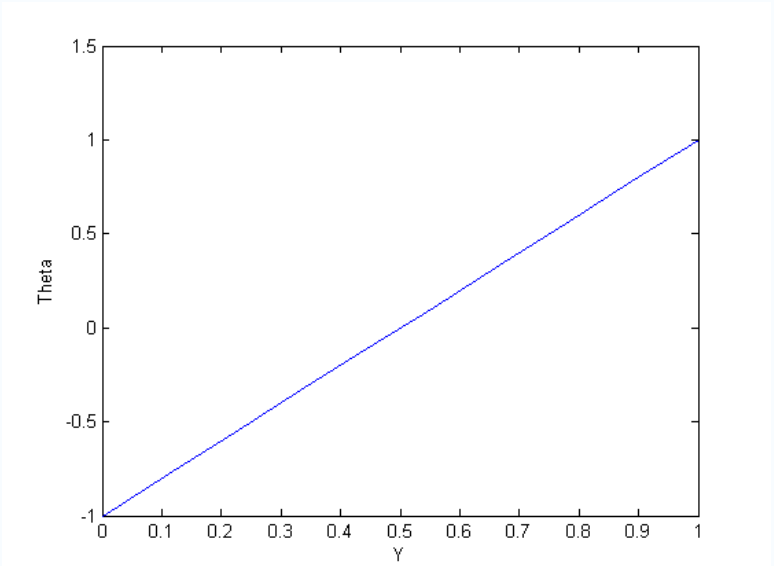

b) $\xi=-1$, In=5

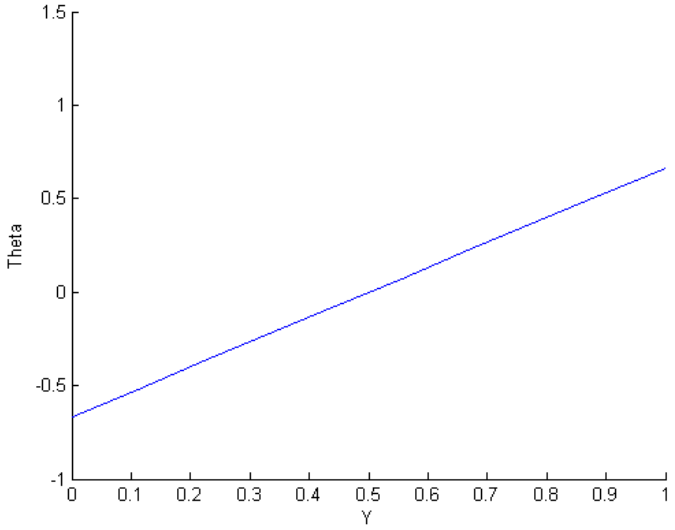

c) ξ=-1, In=10

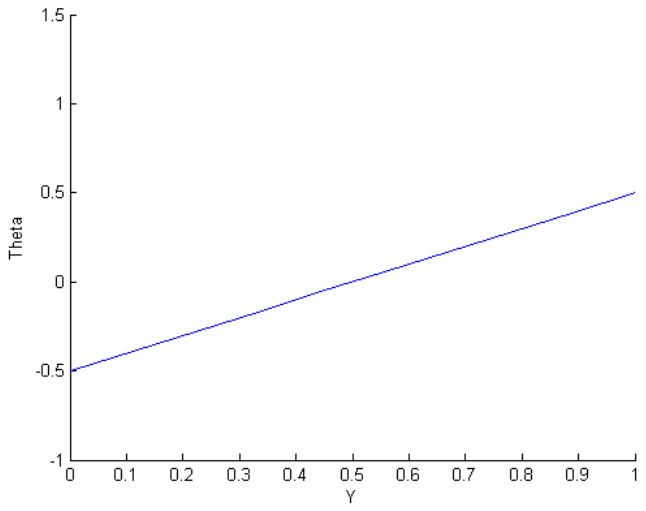

d) ξ=0, In=0

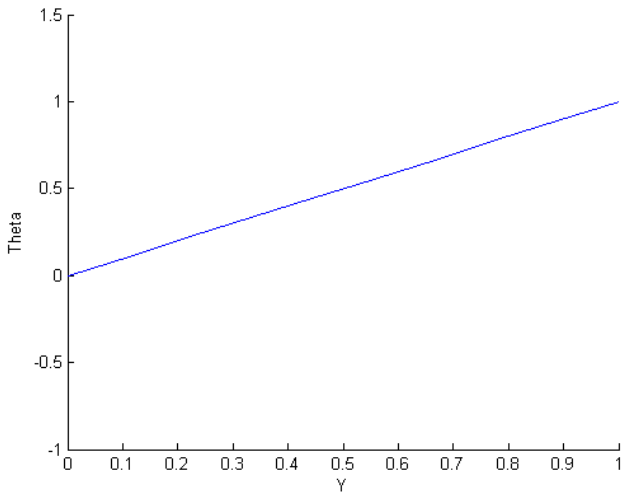

e) ξ=0, In=5

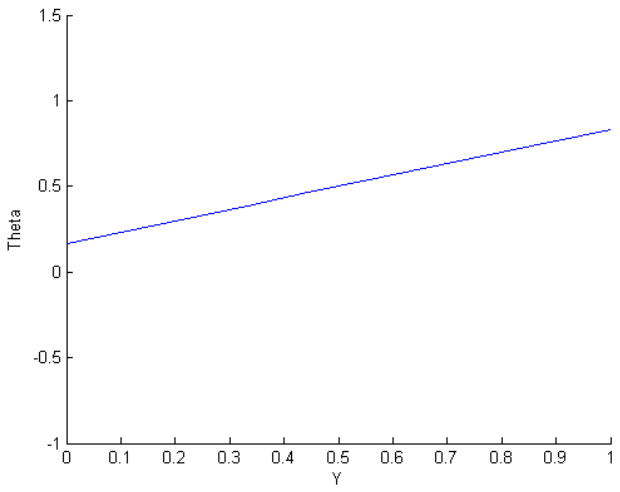

f) ξ=0, In=10

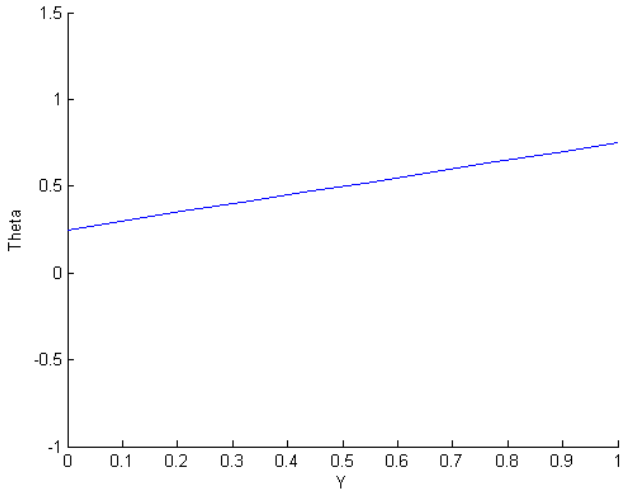

g) ξ=1, In=0,5,10

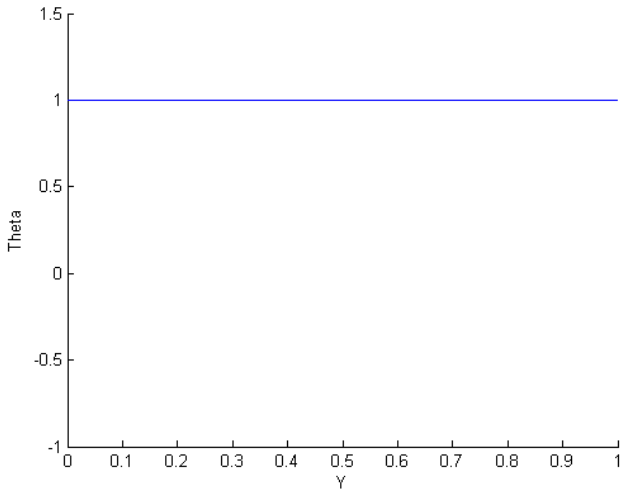

Now the cumulative graph for constant $\beta_v Kn$ is drawn with varying In. the highlighted points denote the points from those obtained by Chen and Wang.

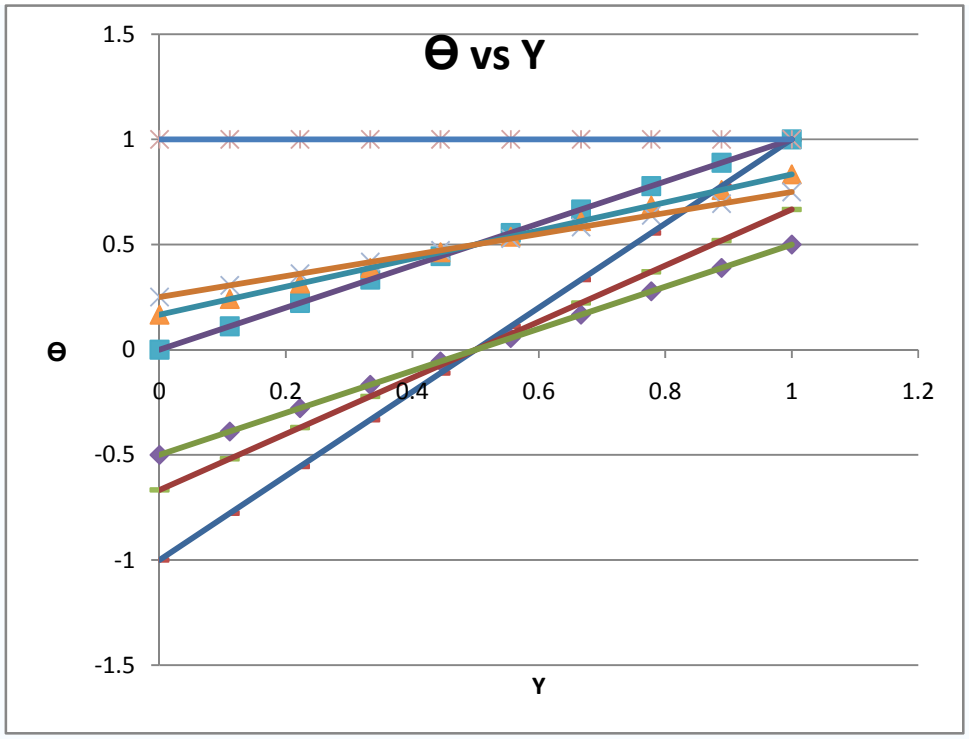

Fig.B

The results for velocities are as shown below:

Constant In=1.667 and β_vKn varies as 0,0.05,1 as ξ varies as -1,0,1.

Result obtained from Matlab 7.0

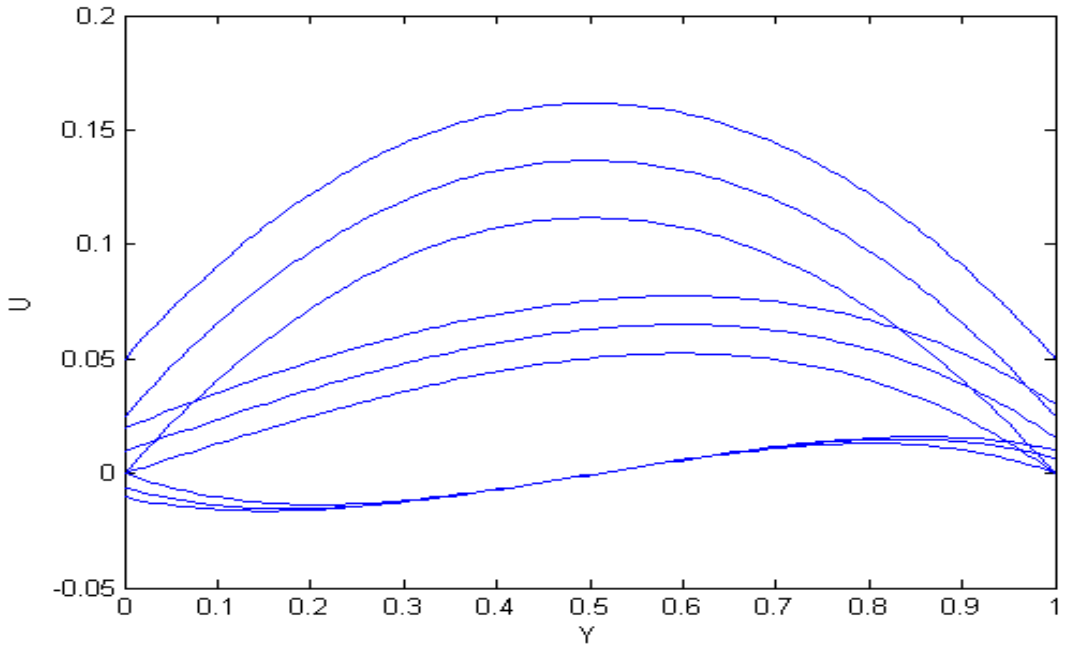

Fig.C

Constant $\beta_v Kn=0.05$ and In varies as 0,5,10 and ξ varies as -1,0,1.

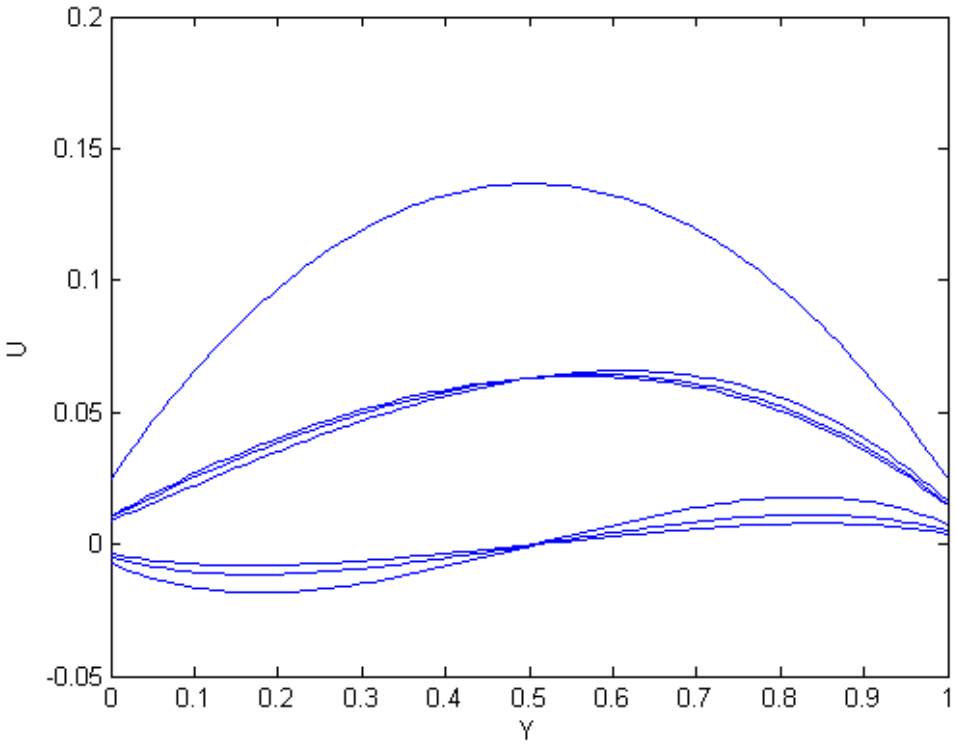

Fig.D

Results validated. The highlighted points represent results from Chen and Wang.

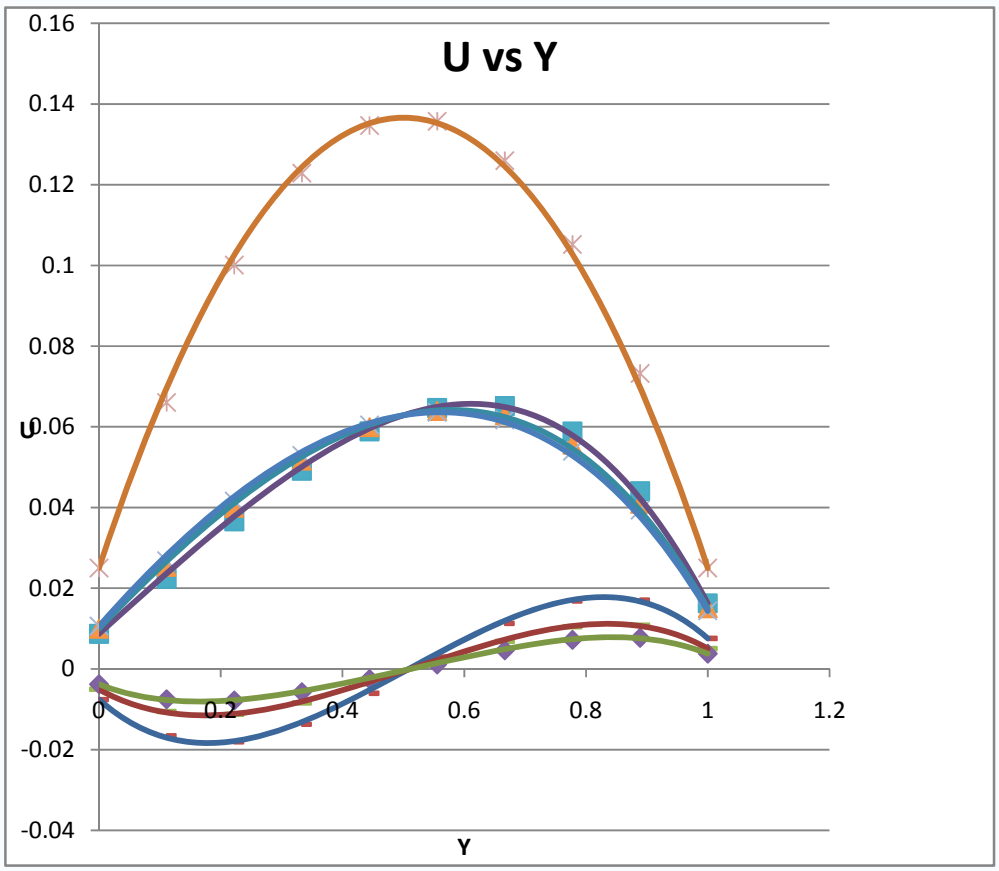

The nusselt no. as well as the volume flow rate were plotted and validated with that provided by Chen and Wang.

M vs β_vKn

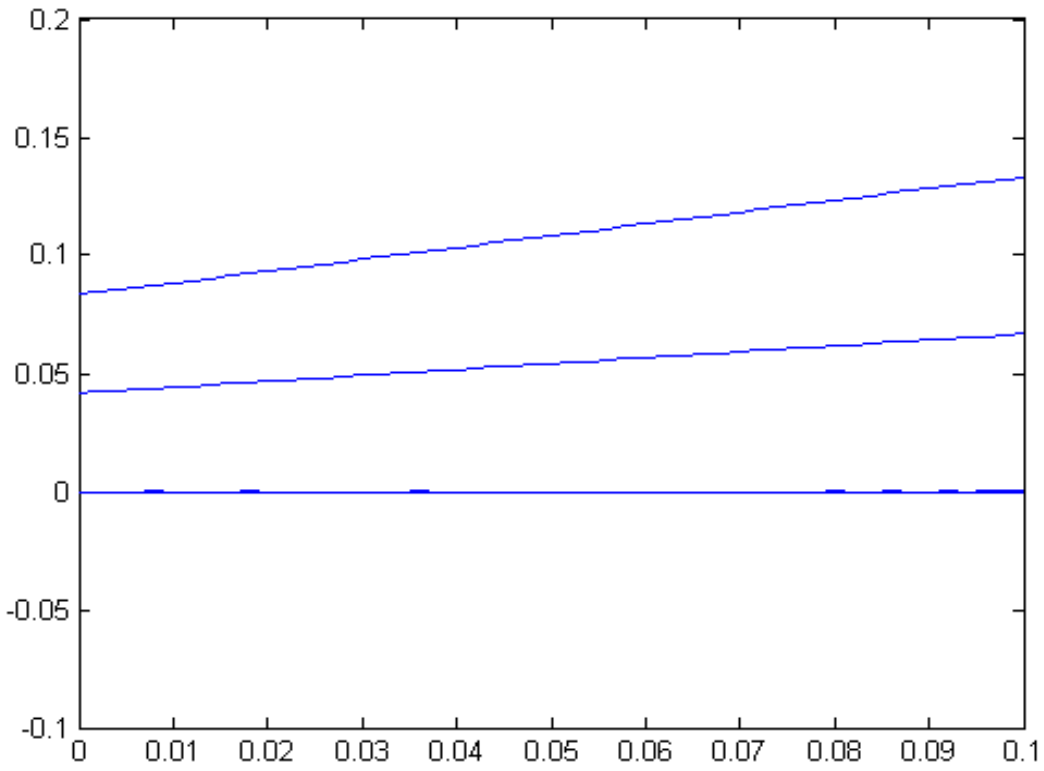

Fig.E

Nu vs β_vKn

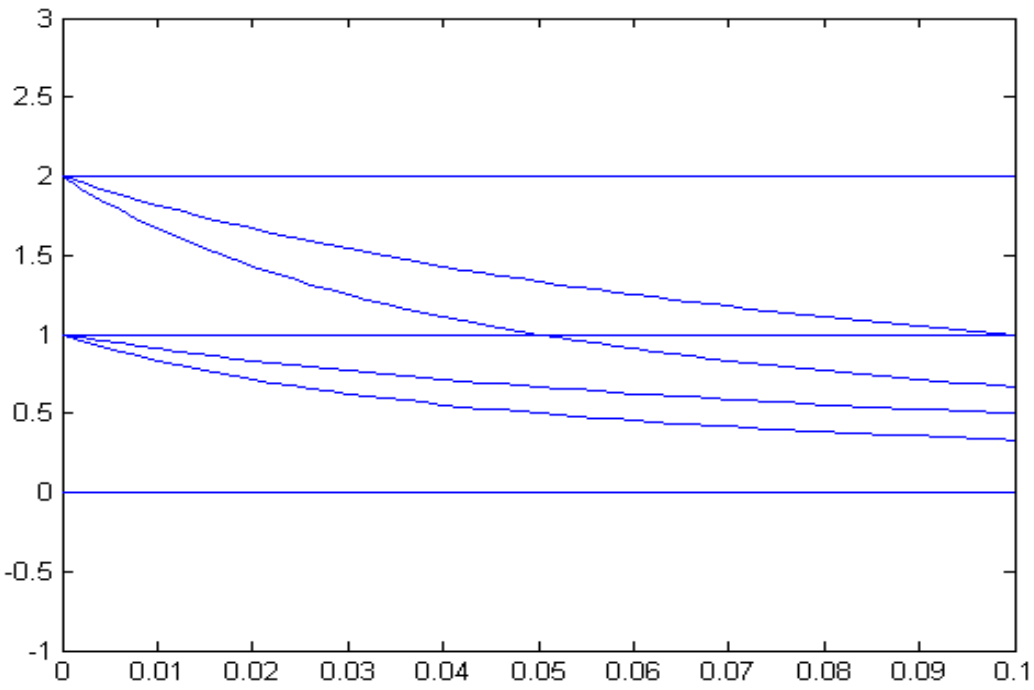

Fig.F

Results and conclusions drawn:

The present parametric study has been performed over the reasonable ranges $0 \leq \beta_v Kn \leq 0.1$ and $0 \leq In \leq 10$. The product β_vKn represents a measure of the departure from the continuum regime, while *In* represents a property of the fluid-wall interaction. The select reference values of β_vKn and *In* for the analysis are 0.05 and 1.667, respectively. In Figs. 2,3,4, we check the results with those for the case $\beta_v Kn=0$ obtained by Aung [8] and with those for a physically impossible case $In=0$(F_t=2). Note that the solutions (10),(11) for $\beta_v Kn=0$ can reduce to

$$\Theta(Y) = (1-\xi)Y + \xi, \qquad (15)$$

$$U(Y) = \frac{(\xi-1)}{6}Y^3 - \frac{\xi}{2}Y^2 + \frac{(2\xi+1)}{6}Y. \qquad (16)$$

Figure A & B shows that, except for the case of symmetric heating (ξ=1), the increase in β_vKn or in *In* leads to large temperature jump and small temperature variation with *Y*. All of the effects increase with the decrease of the wall-ambient temperature difference ratio. In Fig. 3, it is found that the increase in $\beta_v Kn$ leads to the increase in $|U|$. The parameter *In* also influences the flow excluding the case ξ=1. For ξ=0 and –1, the effect of fluid-wall interaction is to horizontally shift the velocity profile to the cooler-wall side and to reduce the fluid velocity, respectively. It is worth noting that as ξincreases, the slip induced by the rarefaction effect increases, but the slip induced by fluid-wall interaction effect decreases.

From Fig. E, it is found that the volume flow rate *M* is a monotone increasing function of β_vKn excluding the case ξ=–1. Furthermore, such rarefaction effect increases with the increase of the value ofξ. It should be noted that as shown in Fig. 3(b), the value of $\int_0^1 UdY$ appears to keep a constant for an assigned value of *In*. The parameter *In*, therefore, exerts no influence on the volume flow rate *M*. We may recall that the physically impossible case *In*=0 only provides the comparative base for the effect of fluid-wall interaction. From Fig.F, we may, therefore, conclude that, except for the case ξ=1, the heat transfer rate obviously decreases with the increases of the values of β_vKn and *In*. Moreover, the effects increase with the decrease of the wall-ambient temperature difference ratio.

b) Developing layer Analysis:

Now a general natural convection is considered which is analysed without the assumption of hydrodynamically or thermally fully developed. This analysis is done to determine the length of the region after which the flow becomes hydrodynamically fully developed. In reality, it is expected that the influences of the developing region are likely to alter the free convection heat transfer characteristics in a vertical microchannel to a significant extent. The underling implications might appear to be somewhat intuitive in nature, but are by no means obvious, primarily because of an interesting and non-trivial interplay between the boundary layer growth in the developing region and the micro-scale effects manifested through wall slippage and temperature jump conditions at the gas-solid interface. The situation gets further complicated by the fact that the thermo-physical properties tend to change significantly with changes in temperature, and cannot be taken as constants for the sake of obtaining closed-form solutions of the associated mathematical problem, at the cost of the practical reliability of the model predictions. To the best of our knowledge, these issues are yet to be comprehensively addressed in the context of free convective heat transfer in vertical microchannels.

Mathematical Remodelling:

A vertical parallel plate microchannel, along with the coordinate system adopted to analyze the flow and heat transfer characteristics of the same, is depicted. The height (H) of the channel is considered to be much larger as compared to its width (D), so as to obtain a fully developed flow in the downstream of the channel. The flow is considered to be two-dimensional. The temperature of the walls of the channel is considered to be uniform at T_w, which is higher than the free stream temperature, T_∞. Accordingly, an upward buoyancy induced flow is generated in the channel. Both ends of the channel are open to the ambient with a temperature of T_∞. The effects of compressibility are neglected in the typical low-speed micro-flows addressed in this study, and only the laminar regimes of flow are considered.

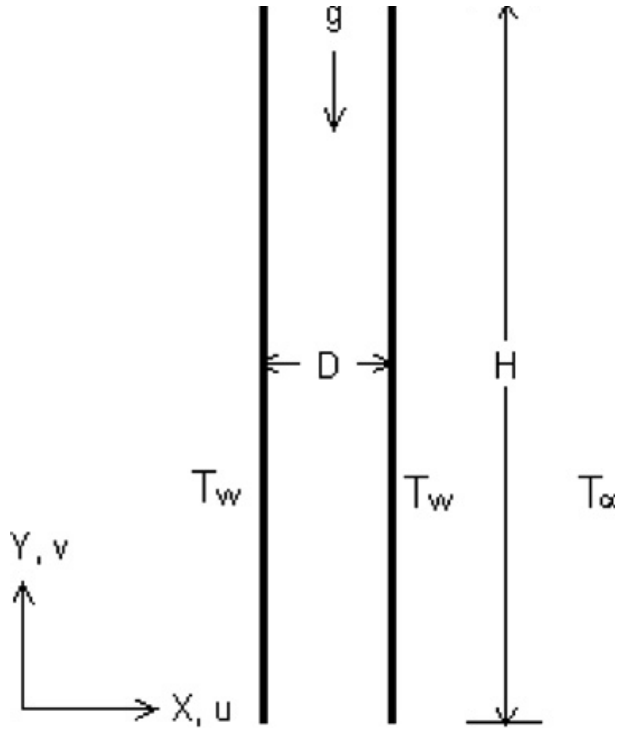

Fig.X Geometry of vertical channel and coordinate system with associated velocity components.

The governing equations of mass, momentum and energy conservation for steady, laminar and incompressible flow with temperature dependent thermo-physical properties [9], appropriate to the analysis of the physical problem described as above, can be written as follows:

Continuity:

$$\frac{\partial(\rho u)}{\partial x} + \frac{\partial(\rho v)}{\partial y} = 0 \qquad \text{Eq.(17)}$$

***X*-momentum:**

$$\frac{\partial}{\partial x}(\rho uu) + \frac{\partial}{\partial y}(\rho vu) = -\frac{\partial p}{\partial x} + \frac{\partial}{\partial x}\left(\mu \frac{\partial u}{\partial x}\right) + \frac{\partial}{\partial y}\left(\mu \frac{\partial u}{\partial y}\right) \qquad \text{Eq.(18)}$$

***Y*-momentum:**

$$\frac{\partial}{\partial x}(\rho uv)+\frac{\partial}{\partial y}(\rho vv)=-\frac{\partial p}{\partial y}+\frac{\partial}{\partial x}\left(\mu\frac{\partial v}{\partial x}\right)+\frac{\partial}{\partial y}\left(\mu\frac{\partial v}{\partial y}\right)+S_v \quad \text{Eq.(19)}$$

$S_v = \rho\, g\, \beta\, (T - T_\infty)$

Energy:

$$\rho_0 c\left(u\frac{\partial T}{\partial x}+v\frac{\partial T}{\partial y}\right)=k\frac{\partial^2 T}{\partial y^2}+\mu\left\{2\left[\left(\frac{\partial u}{\partial x}\right)^2+\left(\frac{\partial v}{\partial y}\right)^2\right]+\left(\frac{\partial u}{\partial y}+\frac{\partial v}{\partial x}\right)^2\right\}$$

$+\boldsymbol{k}\frac{\partial^2 T}{\partial x^2}$ Eq.(20)

The boundary conditions employed for the solution of Eq.(17),(18),(19),(20) are as follows:

Inlet

$u=0,\ \ v=v_{avg}\ ,\ T = T_\infty$

Outlet

$\frac{\partial u}{\partial y}=0,\ \ \frac{\partial v}{\partial y}=0,\ \ \frac{\partial T}{\partial y}=0$

Walls: (Slip flow)

$u=0,\ v_{s=}\ \frac{2-\sigma}{\sigma}\ \mathrm{KnD}\ \ [\frac{\partial v}{\partial x}]_w$

$T_S=T_W+\frac{2-\sigma}{\sigma}\ \frac{2\gamma}{\gamma+1}\ \mathrm{KnD}\ \ [\frac{1}{Pr}\frac{\partial T}{\partial x}]_w$

Looking at the momentum equations, Eq. (18) and Eq. (19) we realize that these can not be discretised and solved as per other partial differential equations. Hence a coupling method knows famously as SIMPLE (Semi Implicit Method for Pressure Linked Equations) algorithm is adopted.

Simple Algoritm in brief:

- Problem occurs:
  - The convective terms of the momentum equation contain non-linear quantities.
  - All three equations are coupled. The most complex issue to resolve is the role played by the pressure.
  - If the correct pressure field is applied in the momentum equations, the resulting velocity field should satisfy continuity.
  - Both the problems associated with the non-linearities in the equation set and the pressure-velocity linkage can be resolved by adopting an iterative solution strategy such as the SIMPLE algorithm of Patankar and Spalding (1972).

1. Staggered grid

- The finite volume method starts with the discretisation of the flow domain and of the relevant transport equations.
- Assuming a highly irregular "checker-board" pressure field:

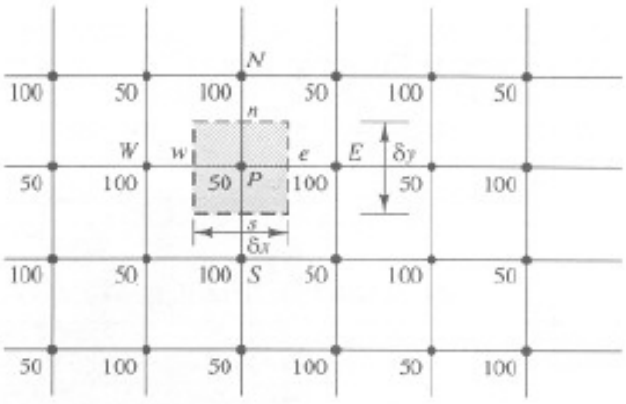

Fig. A Pressure checker board arrangement

- It seems logical to define the velocities at the same locations as the scalar variables such as pressure, temperature etc. If the velocities and pressures are both defined at the nodes of an ordinary control volume, a highly non-uniform pressure field can act like a uniform field in the discritised momentum equations.
- If the linear interpolation is used:
  - The pressure gradient in the u-momentum equation:

$$\frac{\partial p}{\partial x} = \frac{p_e - p_w}{\delta x} = \frac{\left(\frac{p_E + p_P}{2}\right) - \left(\frac{p_P + p_W}{2}\right)}{\delta x} = \frac{p_E - p_W}{2\delta x}$$

  - The pressure gradient in the v-momentum equation:

$$\frac{\partial p}{\partial y} = \frac{p_N - p_S}{2\delta y}$$

  - Substituting the appropriate values, we find that all the discretised gradients are zero at all the nodal points.
  - This behaviour is obviously non-physical.
- A "staggered grid" for the velocity components (Harlow and Welch, 1965) is used:
  - Scalar variables, such as pressure, density, temperature etc., are evaluated at ordinary nodal points.
  - Velocity components and other vector quantities are calculated on staggered grids centred around the cell faces:

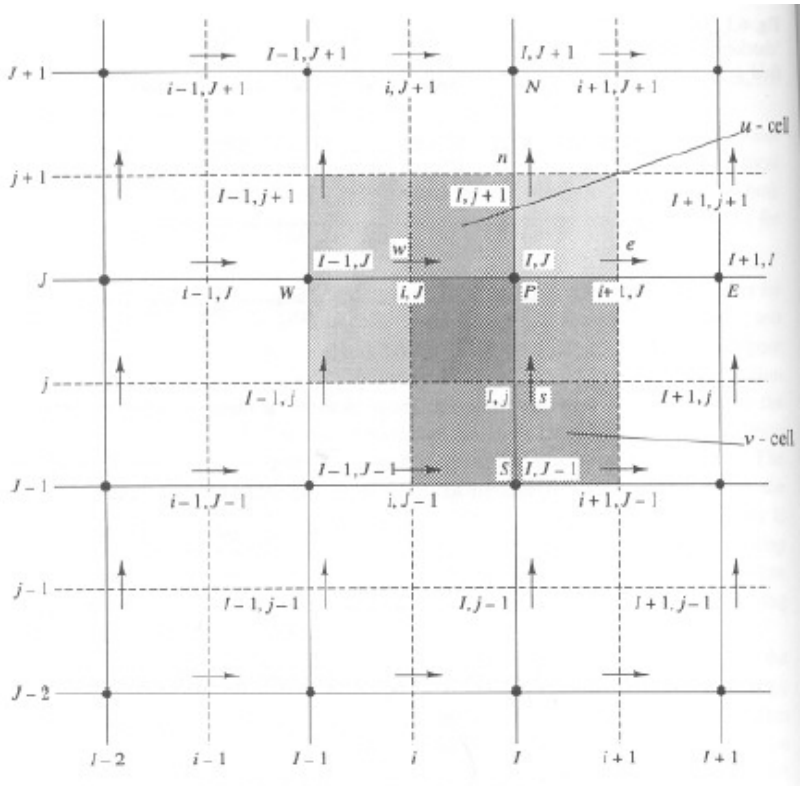

Fig A staggered grid arrengement

- A new system of notation is introduced based on a numbering of grid lines and cell faces. The control volumes for *u* and *v* are different from the scalar control volumes.
- The pressure gradient terms are given by:

$$\frac{\partial p}{\partial x} = \frac{p_E - p_W}{\delta x_u}$$

and

$$\frac{\partial p}{\partial y} = \frac{p_N - p_S}{\delta y_v}$$

where δx_u is the width of the *u*-control volume and δy_v is the width of the *v*-control volume.

- The staggering of the velocity avoids the unrealistic behaviour of the discretised momentum equation for spatially oscillating pressure and generates velocities at exactly the locations where they are required for the scalar transport (i.e. no interpolation is needed).

2. The momentum equations

- If the pressure field is known, the discretisation of velocity equations and the subsequent solution procedure is similar to that of a scalar equation.
  - ✓ Scalar nodes, located at the intersection of two grid lines, are identified by two capital letters: e.g. point *P* is denoted by (*I, J*).

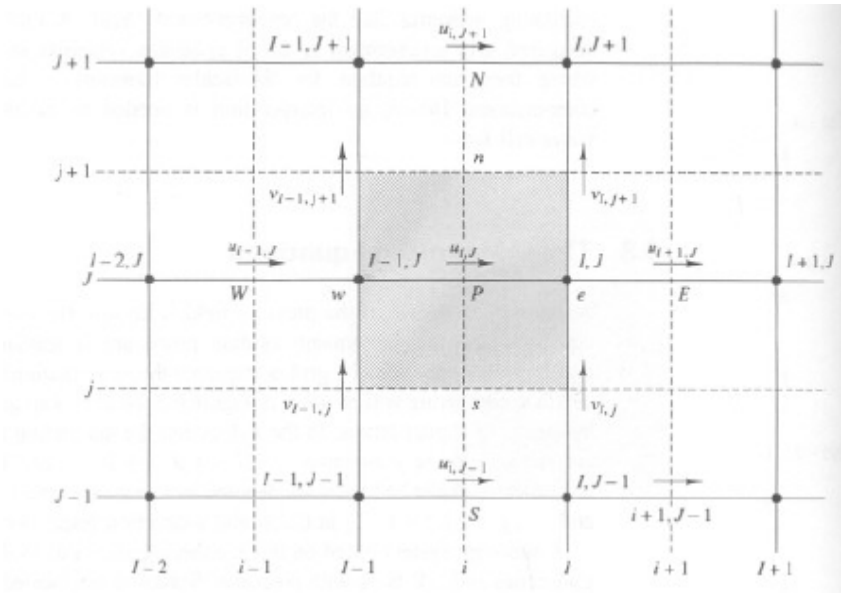

Fig. A u-control volume showing adjacent velocity components.

- The *u*-velocities are stored at the *e*- and *w*-cell faces of a scalar control volume: e.g. the *w*-face of the cell around point *P* is identified by (*i, J*) and the *s*-face is given by (*I, j*).
  - Expressed in the new co-ordinate system, the discretised *u*-momentum equation for the velocity at location (*i*, *J*) is:

    $$a_{i,J}u_{i,J} = \sum a_{nb}u_{nb} - \frac{p_{I,J} - p_{I-1,J}}{\delta x_u}\Delta V_u + \bar{S}\Delta V_u$$

    or

    $$a_{i,J}u_{i,J} = \sum a_{nb}u_{nb} + \left(p_{I-1,J} - p_{I,J}\right)A_{i,J} + b_{i,J}$$

    where ΔV_u is the volume of the u-cell, $b_{i,J} = \bar{S}\Delta V_u$ is the momentum source term, $A_{i,J}$ is the cell face area of the *u*-control volume.
  - In the new numbering system, the *E, W, N* and *S* neighbours involved in the summation $\sum a_{nb}u_{nb}$ are (*i-1,J*), (*i+1,J*), (*i,J+1*) and (*i,J-1*).
  - The values of coefficients $a_{i,J}$ and a_{nb} may be calculated with any of the differencing methods (upwind, hybrid, QUICK) suitable for convection-diffusion problems.
  - The values of *F* and *D* for each of the faces of the *u*-control volume:

    $$F_w = (\rho u)_w = \frac{F_{i,J} + F_{i-1,J}}{2} = \frac{1}{2}\left[\left(\frac{\rho_{I,J} + \rho_{I-1,J}}{2}\right)u_{i,J} + \left(\frac{\rho_{I-1,J} + \rho_{I-2,J}}{2}\right)u_{i-1,J}\right]$$

    $$F_e = (\rho u)_e = \frac{F_{i+1,J} + F_{i,J}}{2} = \frac{1}{2}\left[\left(\frac{\rho_{I+1,J} + \rho_{I,J}}{2}\right)u_{i+1,J} + \left(\frac{\rho_{I,J} + \rho_{I-1,J}}{2}\right)u_{i,J}\right]$$

    $$F_s = (\rho v)_s = \frac{F_{I,j} + F_{I-1,j}}{2} = \frac{1}{2}\left[\left(\frac{\rho_{I,J} + \rho_{I,J-1}}{2}\right)v_{I,j} + \left(\frac{\rho_{I-1,J} + \rho_{I-1,J-1}}{2}\right)v_{I-1,j}\right]$$

    $$F_n = (\rho v)_n = \frac{F_{I,j+1} + F_{I-1,j+1}}{2} = \frac{1}{2}\left[\left(\frac{\rho_{I,J+1} + \rho_{I,J}}{2}\right)v_{I,j+1} + \left(\frac{\rho_{I-1,J+1} + \rho_{I-1,J}}{2}\right)v_{I-1,j+1}\right]$$

    $$D_w = \frac{\Gamma_{I-1,J}}{x_i - x_{i-1}}$$

    $$D_e = \frac{\Gamma_{I,J}}{x_{i+1} - x_i}$$

    $$D_s = \frac{\Gamma_{I-1,J} + \Gamma_{I,J} + \Gamma_{I-1,J-1} + \Gamma_{I,J-1}}{4(y_J - y_{J-1})}$$

    $$D_n = \frac{\Gamma_{I-1,J+1} + \Gamma_{I,J+1} + \Gamma_{I-1,J} + \Gamma_{I,J}}{4(y_{J+1} - y_J)}$$

    - Scalar variables or velocity components are not available at a *u*-control volume cell face.
    - A suitable two- or four-point average is formed over the nearest points where values are available.
- Similarly, the *v*-momentum equation:

$$a_{I,j}v_{I,j} = \sum a_{nb}v_{nb} + \left(p_{I,J-1} - p_{I,J}\right)A_{I,j} + b_{I,j}$$

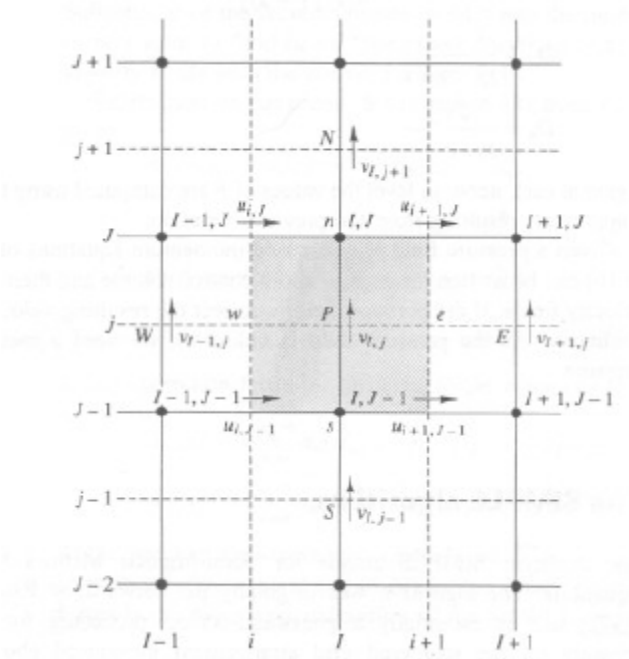

Fig. A v-control volume showing adjacent velocities

- The values of F and D for each of the faces of the v-control volume:

$$F_w = (\rho u)_w = \frac{F_{i,J} + F_{i,J-1}}{2} = \frac{1}{2}\left[\left(\frac{\rho_{I,J} + \rho_{I-1,J}}{2}\right)u_{i,J} + \left(\frac{\rho_{I-1,J-1} + \rho_{I,J-1}}{2}\right)u_{i,J-1}\right]$$

$$F_e = (\rho u)_e = \frac{F_{i+1,J} + F_{i+1,J-1}}{2} = \frac{1}{2}\left[\left(\frac{\rho_{I+1,J} + \rho_{I,J}}{2}\right)u_{i+1,J} + \left(\frac{\rho_{I,J-1} + \rho_{I+1,J-1}}{2}\right)u_{i+1,J-1}\right]$$

$$F_s = (\rho v)_s = \frac{F_{I,j-1} + F_{I,j}}{2} = \frac{1}{2}\left[\left(\frac{\rho_{I,J-1} + \rho_{I,J-2}}{2}\right)v_{I,j-1} + \left(\frac{\rho_{I,J} + \rho_{I,J-1}}{2}\right)v_{I,j}\right]$$

$$F_n = (\rho v)_n = \frac{F_{I,j} + F_{I,j+1}}{2} = \frac{1}{2}\left[\left(\frac{\rho_{I,J} + \rho_{I,J-1}}{2}\right)v_{I,j} + \left(\frac{\rho_{I,J+1} + \rho_{I,J}}{2}\right)v_{I,j+1}\right]$$

$$D_w = \frac{\Gamma_{I-1,J-1} + \Gamma_{I,J-1} + \Gamma_{I-1,J} + \Gamma_{I,J}}{4(x_I - x_{I-1})}$$

$$D_e = \frac{\Gamma_{I,J-1} + \Gamma_{I+1,J-1} + \Gamma_{I,J} + \Gamma_{I+1,J}}{4(x_{I+1} - x_I)}$$

$$D_s = \frac{\Gamma_{I,J-1}}{y_j - y_{j-1}}$$

$$D_n = \frac{\Gamma_{I,J}}{y_{j+1} - y_j}$$

- During each iteration level, the values of F are computed using the u- and v-velocity components resulting form the previous iteration.
- Given a pressure field p, discretised momentum equations can be written for each u-

and *v*-control volume and then solved to obtain the velocity fields. If the pressure field is correct, the resulting velocity field will satisfy continuity.

3. The Semi-Implicit Method for Pressure-Linked Equation (SIMPLE) algorithm

- The algorithm was originally put forward by Patankar and Spalding (1972) and is essentially a guess-and-correct procedure for the calculation of pressure on the staggered grid.
- Algorithm:
  - To initiate the SIMPLE calculation process a pressure field p^* is guessed.
  - Discretised momentum equations are solved using the guessed pressure field to yield velocity components u^* and v^*:

$$a_{i,J}u^*_{i,J} = \sum a_{nb}u^*_{nb} + \left(p^*_{I-1,J} - p^*_{I,J}\right)A_{i,J} + b_{i,J}$$

$$a_{I,j}v^*_{I,j} = \sum a_{nb}v^*_{nb} + \left(p^*_{I,J-1} - p^*_{I,J}\right)A_{I,j} + b_{I,j}$$

  - Define the correction p' and the correct pressure field p:

$$p = p^* + p'$$

  - Define the velocity corrections and the correct velocities:

$$u = u^* + u'$$

$$v = v^* + v'$$

  - Solve pressure correction equation to obtain the pressure correction.

$$a_{I,J}p'_{I,J} = a_{I+1,J}p'_{I+1,J} + a_{I-1,J}p'_{I-1,J} + a_{I,J+1}p'_{I,J+1} + a_{I,J-1}p'_{I,J-1} + b'_{I,J}$$

with

$$a_{I,J} = a_{I+1,J} + a_{I-1,J} + a_{I,J+1} + a_{I,J-1}$$

$a_{I+1,J}$	$a_{I-1,J}$	$a_{I,J+1}$	$a_{I,J-1}$	$b'_{I,J}$
$(\rho dA)_{i+1,J}$	$(\rho dA)_{i,J}$	$(\rho dA)_{I,j+1}$	$(\rho dA)_{I,j}$	$(\rho u^* A)_{i,J} - (\rho u^* A)_{i+1,J} + (\rho v^* A)_{I,j} - (\rho v^* A)_{I,j+1}$

  - The pressure correction equation is susceptible to divergence unless some under-relaxation is used during the iterative process:

$$p^{new} = p^* + \alpha_p p'$$

where α_p is the pressure under-relaxation factor.

  - The iteratively improved velocity components u^{new} and v^{new} are:

$$u^{new} = \alpha_u u + (1-\alpha_u)u^{(n-1)}$$

$$v^{new} = \alpha_v v + (1-\alpha_v)v^{(n-1)}$$

where α_u and α_v are the *u*- and *v*-velocity under-relaxation factors with values between 0 and 1; *u* and *v* are the corrected velocity components without relaxation and $u^{(n-1)}$ and $v^{(n-1)}$ are their values obtained in the previous iteration.

  - Process till convergence.

It may be expressed in the form of a flowchart as shown below.

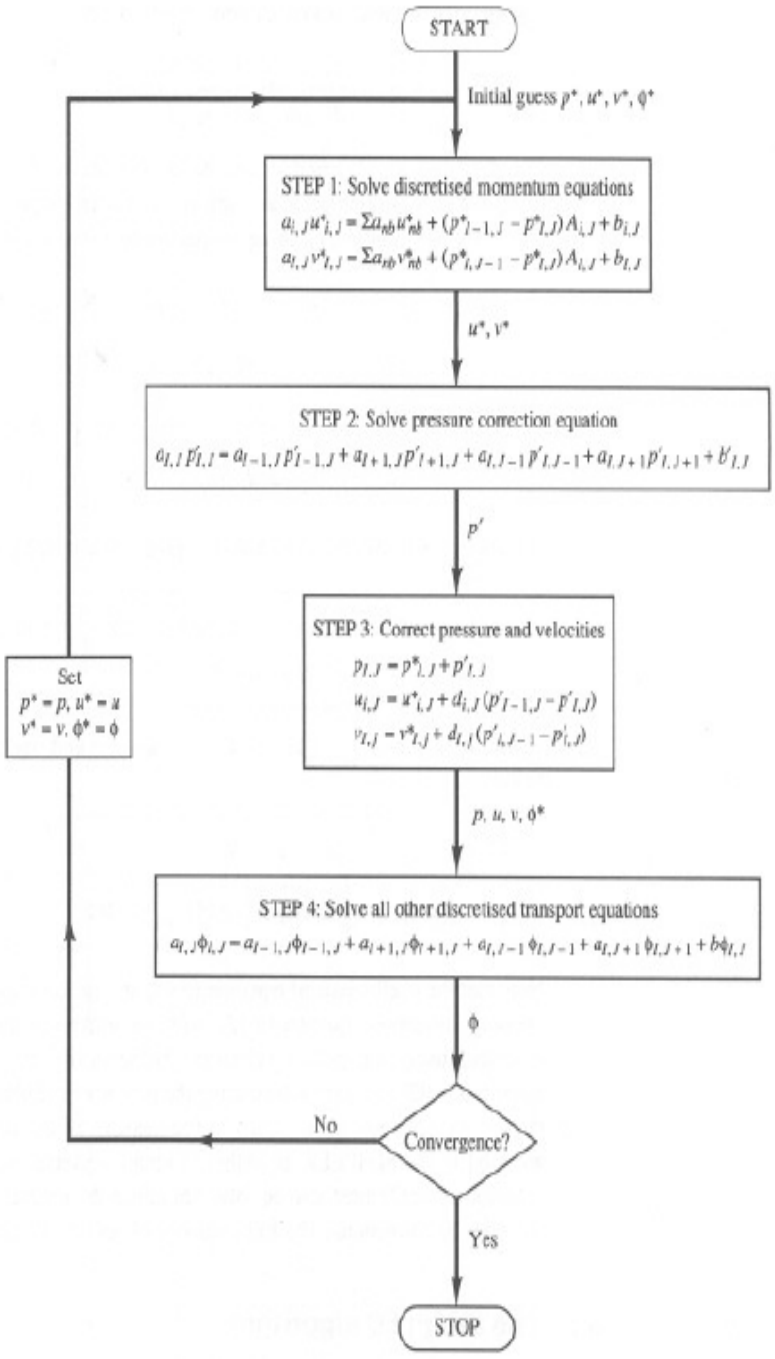

Fig. SIMPLE Algorithm.

Same algorithm is followed and here the Temperature (T) is the φ from the flowchart. A (40*5000) grid is considered. An under relaxation factor of 0.2 is used. Tolerance limit is kept at 10^{-5}.

Results and conclusions:

The general analysis is found to validate the hydrodynamically developed flow analysis after a certain entrance length. The 'v' (fig.X) velocity is found to remain constant with height of the channel after certain length. The horizontal velocity factor 'u' (fig.X) along the channrl width vanishes after certain length.

The Temperature T is found to remain constant with height after the entrance length. To validate the result a curve was plotted for the velocity 'v' vs the channel width after the entrance length and it was compared with that obtained above for hydrodynamically fully developed flow.

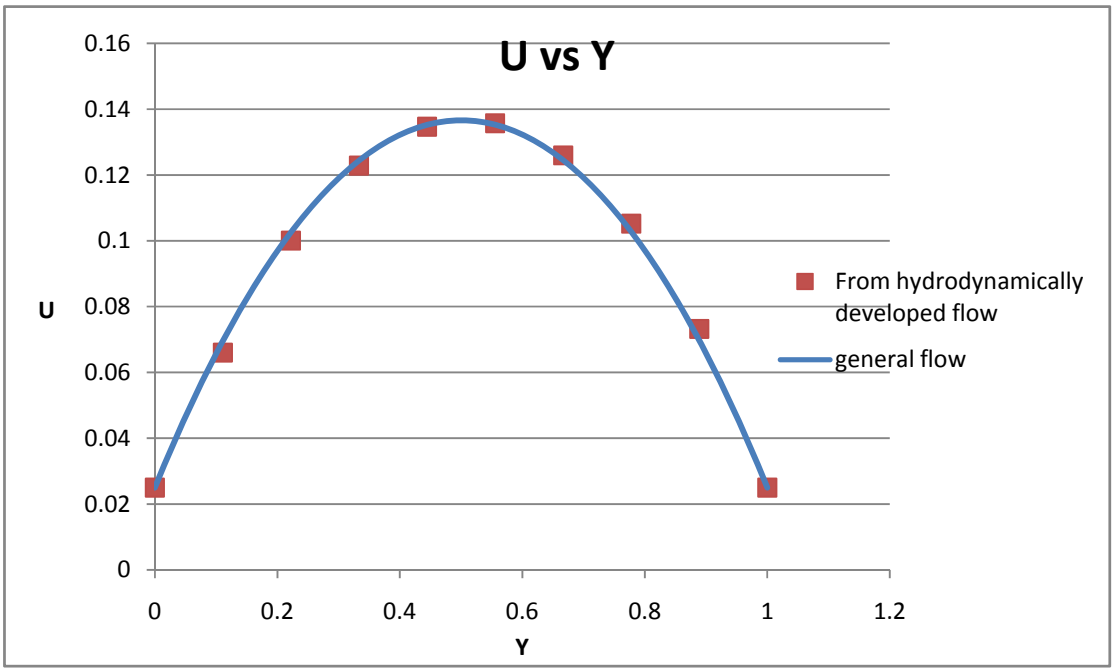

6. Conclusions:

An analytical study on the slip-flow natural convection in a parallel-plate microchannel with uniform but not necessarily symmetric wall temperature distributions has been made. Results of present study show that the effects of rarefaction and fluid-wall interaction are important and should be considered for micronatural convective flow and heat transfer problems. Such effects may result in the increase of the volume flow rate and the decrease of the heat transfer rate. As the wall-ambient temperature difference ratio decreases, the effects on the volume flow decreases and those on the heat transfer rate increase. The present analytical studies help the understanding of fluid transport and heat transfer behavior in microchannels and benefit the design of micropumps and microheat exchangers.

From the general analysis we concluded that flow ina microchannel does get hydrodynamically as well thermally fully developed after a certain entrance length. Thou the flow and properties in the entrance length can not be neglected, for rarefied gaseous micronatural convection (typically low-speed flow and low Prandtl- number fluid) such assumptions can be considered valid.

7. Scope for future research:

- Further analysis may be carried out using modern day advanced CFD software to exactly **determine the entrance length** after which the flow in a microchannel can be considered as hydodynamically as well as thermally fully developed.

- Analysis may be done to determine the exact **speed** and the value of **Prandtl number** below which such assumptions become valid.

- Different conditions such as isothermally maintained walls or insulated walls may be explored and the results compared to determine the optimum heat dissipation method.

8. Nomenclature:

b = channel width

Br = Brinkman number, $\mu U_c^2/k(T_1-T_0)$

c, c_v = specific heats at constant pressure and constant volume, respectively

F_t, F_v = thermal and tangential momentum accommodation coefficients, respectively

g = gravitational acceleration

In = fluid-wall interaction parameter, β_t/β_v

k = thermal conductivity

Kn = Knudsen number, λ/b

l= channel length

l^* = entrance length (Fig.)

m = volume flow rate

M = dimensionless volume flow rate, Eq. (13)

Nu = dimensionless heat transfer rate (Nusselt number), Eq. (13)

p = pressure

$\hat{p}$ = pressure defect, $p-p_h$

p_h = hydrostatic pressure

Pr = Prandtl number, $\mu c/k$

q = heat transfer rate

Ra = Rayleigh number, $\rho_0 c U_c b/k$

T = temperature

u,v = velocity components in x,y directions

U = dimensionless velocity component in x direction, Eq. (6)

U_c = characteristic velocity, Eq. (6)

x,y = rectangular coordinate system

X,Y = dimensionless rectangular coordinate system, Eq. (6)

β= thermal expansion coefficient

β_t, β_v = dimensionless variables, Eq. (9)

γ_s = ratio of specific heats, c/c_v

λ = molecular mean free path

μ = dynamic viscosity

Θ = dimensionless temperature, Eq. (6)

ξ= wall-ambient temperature difference ratio, Eq. (9)

μ = density

1 = hotter-wall values

2 = cooler-wall values

0 = inlet properties of the fluid

9. References:

1. Schaaf, S.A., and Chambre, P.L., 1961, *Flow of Rarefied Gases*, Princeton University Press, Princeton. first citation in article
2. Arkilic, E. B., Breuer, K. S., and Schmidt, M. A., 1994, "Gaseous Flow in Microchannels, Application of Micro-Fabrication to Fluid Mechanics," ASME FED, **197**, pp. 57–66. first citation in article
3. Liu, J.Q., Tai, Y.C., and Ho, C.M., 1995, "MEMS for Presure Distribution Studies of Gaseous Flow in Microchannels," *Proceedings, IEEE Micro Electro Mechanical Systems*, pp. 209–215. first citation in article
4. Larrode, F. E., Housiadas, C., and Drossinos, Y., 2000, "Slip-Flow Heat Transfer in Circular Tubes," Int. J. Heat Mass Transfer, **43**, pp. 2669–2680. [Inspec] [ISI] first citation in article
5. Yu, S., and Ameel, T. A., 2001, "Slip-Flow Heat Transfer in Rectangular Microchannels," Int. J. Heat Mass Transfer, **44**, pp. 4225–4234. [Inspec] [ISI] first citation in article
6. Elenbaas, W., 1942, "Heat Dissipation of Parallel Plates by Free Convection," Physica (Amsterdam) **9**, pp. 1–28. [ISI] first citation in article
7. Gebhart, B., Jaluria, Y., Mahajan, R.L., and Sammakia, B., 1988, *Buoyancy-Induced Flows and Transport*, Hemisphere, New York, Chap. 14. first citation in article
8. Aung, W., 1972, "Fully Developed Laminar Free Convection Between Vertical Plates," Int. J. Heat Mass Transfer, **15**, pp. 1577–1580. [Inspec] [ISI] first citation in article
9. Kavehpour, H. P., Faghri, M., and Asako, Y., 1997, "Effects of Compressibility and Rarefaction on Gaseous Flows in Microchannels," Numer. Heat Transfer, Part A, **32**, pp. 677–696. [ISI] first citation in article
10. Bejan, A., 1995, *Convection Heat Transfer*, Wiley, New York, Chap. 4. first citation in article

11. Eckert, E.R.G., and Drake, R.M., Jr., 1972, *Analysis of Heat and Mass Transfer*, McGraw–Hill, New York, Chap. 11. first citation in article
12. Rohsenow, W.M., and Hartnett, J.P., 1973, *Handbook of Heat Transfer*, McGraw–Hill, New York, Chap. 9. first citation in article
13. Goniak, R., and Duffa, G., 1995, "Corrective Term in Wall Slip Equations for Knudsen Layer," J. Thermophys. Heat Transfer **9**, pp. 383–384. [ISI] first citation in article
14. C.-K. Chen and H.C. Weng, Natural convection in a vertical microchannel, *J. Heat Transfer* **127** (2005), pp. 1053–1056.
15. Biswal L., Som S.K. , Chakrabarty S. , Effects of entrance region transport processes on free convection slip flow in vertical microchannels with isothermally heated walls. Int.J. Heat & Mass Transfer.
16. Versteeg.H.K. , Malalasekara. W, An introduction to computational fluid dynamics- The Finite Volume Method.
17. www.cfd-online.com
18. www.wikipedia.org